INTERNATIONAL CONFERENCE ON LIGHTNING PROTECTION
33rd International Conference on Lightning Protection
25 - 30 September 2016
Estoril, Portugal

Time-Frequency Features of Lightning-generated Electric Fields Appliying the Local Polynomial Fourier Transform (LPFT)

Herbert E. Rojas *+
* Universidad Distrital Francisco José de Caldas
Electromagnetic Compatibility and Interference Res. Group
Bogotá, Colombia
herojasc@udistrital.edu.co
+ Electromagnetic Compatibility Research Group (EMC-UNC)
Universidad Nacional de Colombia
Department of Electrical Engineering

Camilo A. Cortés; Francisco J. Román
Electrical and Electronic Engineering Department
Universidad Nacional de Colombia
+ Electromagnetic Compatibility Research Group (EMC-UNC)
Bogotá, Colombia
caacortesgu@unal.edu.co
fjromanc@unal.edu.co

***Abstract*— In the last two decades, various lightning events have been analyzed using mathematical and signal processing techniques. In this paper, electric field waveforms radiated by negative first and subsequent strokes were analyzed using the Local Polynomial Fourier Transform (LPFT). The analysis provided by LPFT shows the instantaneous frequency (IF) of the signals and its first derivative. The electric field signatures came from a thunderstorm occurred in Bogotá, Colombia. In addition, the return stroke energy concentration is presented in the form of the Local Polinomial Periodogram (LPP). The LPP shows that the return stroke spectrum is distributed in a frequency range with the peak value spread in a specific part of this range. Form the time-frequency analysis provided by LPFT, the energy radiated by negative first return strokes remains in the average frequency range from low frequency (lower than 1 kHz) up to 36 kHz, while the energy radiated by subsequent strokes ranges between 0.5-42 kHz. In addition, for the initial stage and the overshoot region of the transient pulse, the first return stroke signatures present a frequency range slightly higher than those of the subsequent return strokes.**

Keywords- Lightning, electric field records, local polinomial Fourier transform, lightning spectrum, time-frequency analysis

I. INTRODUCTION

Last decades advancements in the measurement of electromagnetic fields generated by lightnings reveal many features [1]. The new developments provide a vast knowledge of lightning electric fields, which is important to identify some parameters and characteristics of the discharge such as lightning currents and its multiplicity. They provide also information for an adequate design and improvement of safety schemes that can be used in lightning detectors and alarms.

From the knowledge of lightning frequency spectra, it is possible to understand the physical processes that take place in different lightning events such as preliminary breakdown pulses, stepped leader, first return strokes, subsequent strokes, and narrow bipolar pulses [2]. In addition, the estimation of the return stroke spectrum can be used to determine the electromagnetic compatibility requirements of equipment and electronic systems.

Through many years, the frequency spectra of different lightning events have been obtained from the lightning electric and magnetic fields radiated by the discharge using a bandwidth measuring system and then time, frequency or hybrid time-frequency domain methods are used to obtain a spectrum. The first results of lighting spectrum were achieved using the conventional Fourier transform (FT) and the short-time Fourier transform (STFT) [3]. With these methods, the frequency spectra obtained were found from low frequencies to a high spread spectrum close to 20 MHz. In addition, the STFT approaches have the advantage that a part of the spectrum can be associated with a specific lightning process [4].

Although the FT and SFTF methods have advantages over the narrowband methods, they have limitations as well. When a time domain signal is analyzed with FT, the major drawback is that the signal has frequency resolution but it lacks time resolution. On the other hand, STFT has the constraint of using fixed bandwidth window, which brings limitations for high frequency and low frequency signals analysis [5].

In the last decade, a significant improvement in the time-frequency analysis of lightning has been achieved by using the wavelet transform (WT) [1], [6]. This method provides a better understanding of different lightning processes. Through the wavelet analysis, it was observed that the power spectrum of a first or subsequent return stroke is not located in a determined value of frequency, as the Fourier analysis reveals, but the spectrum is displaces in a limited frequency range which varies in time. However, the selection process of the mother wavelet is still an issue that needs to be studied.

Recently, to complement these results, time-frequency analyses of lightning phenomena have extended to the application of linear time-frequency representations (TFRs). The Local Polynomial Fourier Transform (LPFT) is a generalized version of the STFT. This transform can be

This work is supported partially by *Universidad Distrital Francisco José de Caldas* through the research project with code 2-5-355-13 and the commission contract N° 000002-2016, and by *Dirección de Investigación sede Bogotá (DIB)* of the Universidad Nacional de Colombia

interpreted as high-order STFT that uses extra parameters to approximate the instantaneous frequency (IF) characteristic of polynomial phase signals (PPSs) [7]. The LPFT has received considerable attention in the last twenty years, and has been used in a variety of applications such as IF estimation, radar imaging, interference suppression in communications, and motion parameter estimation in video sequences [7]–[9].

This paper presents a time-frequency analysis of electric field signals radiated by lightning using the LPFT. The motivation behind this study lies in the fact that the LPFT can provide much better concentration and resolution than the STFT and other signal processing techniques. Moreover, due to its linearity, the LPFT is free from the cross terms common to other TFRs as the Wigner Distribution (WD) [8].

The paper is organized as follows: a review of the LPFT, its definition, properties and relationship with other TFRs is discussed in Section II. Section III gives a brief explanation of the measuring system. The methodology for LPFT application in electric field signals is described in Section IV. Section V presents the results and discussion of the time-frequency analysis for lightning return stroke radiated signals. Finally, some conclusions are drawn in section VI.

II. Local Polynomial Fourier Transform (LPFT)

LPFT is a signal processing technique used to estimate the instantaneous frequency (IF) and the energy concentration of a harmonic complex-value or time varying signal [10]. To approximate the local polynomial function, the LPFT introduces polynomial parameters including the first-order and other higher-order derivatives of the IF of the analyzed signal. The LPFT is a linear TFRs that can be defined as follow [7]:

$$Y_h(\bar{\omega},t)=\int_{-\infty}^{\infty}\rho_h(u)y(t+u)e^{-j\theta(u,\bar{\omega})}du \tag{1}$$

To calculate computationally the LPFT, it is better to use the following definition:

$$Y_h(\bar{\omega},t)=\sum_{n=-\infty}^{\infty}\rho_h(nT_s)y(t+nT_s)e^{-j\theta(u,\bar{\omega})} \tag{2}$$

where $y(t+nT_s)$ is the signal and T_s is the sampling time of the signal. The function $\rho_h(nT_s)$ is a window function of bandwidth h that formalizes the location of fitting with respect to the center point nT_s. The function ρ_h is a finite support function that satisfies some properties:

$$\begin{aligned}&\rho_h(u)\geq 0;\quad \rho(0)=\max_u\rho_h(u)\\&\rho_h(u)\to 0\ \text{ as }\ |u|\to\infty;\quad \int_{-\infty}^{\infty}\rho_h(u)du=1\end{aligned} \tag{3}$$

where $u=nT_s$. In (2) the exponential term $\exp[-j\theta(u,\bar{\omega})]$ is the LPFT kernel function defined as [7]:

$$\theta(u,\bar{\omega})=\omega_1 u+\omega_2\frac{u^2}{2}+\cdots+\omega_m\frac{u^m}{m!} \tag{4}$$

From (4), it is possible to define a set of estimators for the IF and its high order derivatives represented by the vector $\bar{\omega}(t)=\big(\omega_1(t),\omega_2(t),\omega_3(t),\dots,\omega_m(t)\big)$, where $\bar{\omega}\in R^m$, $\omega_1(t)$ is the true value of the IF, $\omega_m(t)$ is the $(m-1)$th derivative of IF and m is the degree of LPFT. According to (2), $Y_h(\bar{\omega},t)$ is a periodic function of $\bar{\omega}(t)$ with periods equal to $2\pi\, s!/T^s$ for $s=1,2,\dots,m$. Thus, the range of values that every estimator from $\bar{\omega}$ can assume is defined by:

$$Y_h(\bar{\omega},t)=Y_h\left(\omega_1+\frac{2\pi}{T},\ \ \omega_2+\frac{4\pi}{T^2},\dots,\omega_m+\frac{4\pi m!}{T^m}\right) \tag{5}$$

In a similar way to the periodogram obtained from STFT, which is defined as an energy distribution over the time-frequency plane $(t-\omega)$, the Local Polynomial Periodogram (LPP) can be interpreted as a time-frequency energy distribution of a signal over the $\big(t-\bar{\omega}(t)\big)$ space [11]. Then the LPP is defined as follow:

$$I_h(\bar{\omega},t)=|Y_h(\bar{\omega},t)|^2 \tag{6}$$

From this definition, the LPP provides the signal energy concentration and can be used to estimate the IF and its derivatives. This property of the LPFT motivates its use as an IF estimator. In the particular case when $m=1$, $Y_h(\bar{\omega},t)$ in (2) corresponds to the definition of the STFT, and $I_h(\bar{\omega},t)$ in (6) is the conventional periodogram.

From (2) and (6) the estimators $\bar{\omega}(t,h)$ are achieved as a solution of the following optimization problem [11]:

$$\bar{\omega}(t,h)=\underset{\bar{\omega}\,\epsilon\,Q\,\subset\,R^m}{arg\max}\, I_h(\bar{\omega},t) \tag{7}$$

where the basic interval of the estimators $\bar{\omega}(t,h)$ is defined by:

$$Q=\{\omega_s:0\leq\omega_s<2\pi\, s!/T^s\ s=1,2,\dots,m\} \tag{8}$$

It is shown that the window bandwidth controls the tradeoff between the bias and variance. Therefore, the estimation accuracy depends on the window bandwidth and the optimization of bandwidth can greatly improve the accuracy. Meanwhile, if the polynomial order m increases it can be improved the accuracy depending on the proper selection of the bandwidth [10]. Into the vector $\bar{\omega}(t,h)$ the estimator related to the IF is $\omega_1(t)$, while $\omega_{s+1}(t)$, $s=1,2,\dots,m$ corresponds to the derivatives of IF. These components converge when:

$$\bar{\omega}(t,h)\to\big(\omega_1(t),\omega_2(t),\omega_3(t),\dots,\omega_m(t)\big)\text{ and }h\to\infty$$

However, when m increases, the complexity of the polynomial exponent in (6) also increases. From these definitions, the LPFT can be interpreted as linear time-frequency representation (TFRs) that shows an energy distribution in $t-\bar{\omega}(t)$ space with a highest level of detail. This definition lies in the fact that the energy concentration of $Y_h(\bar{\omega},t)$ is determined at each time instant.

To determine the values of $\bar{\omega}(t)$ at each time, the local polynomial approximation (LPA) searches the highest energy concentration points in the LPP by means the following optimization problem [11], [12]:

$$\bar{\omega}(t,h)=\underset{\bar{\omega}\,\epsilon\,Q\,\subset\,R^m}{arg\max}\, I_h(\bar{\omega},t) \tag{9}$$

The adequate location of the estimators from the LPA is insured through the window function ρ_h. This function only considers the observations in the neighborhood of a "center" point t.

III. Measuring System

The measuring system used to acquire the vertical electric fields produced by lightning is located in Bogota-Colombia (reference point: 4° 36' N, 74° 5' W) at 2640 m above sea level. The scheme of the measuring station is shown in Fig. 1 [13].

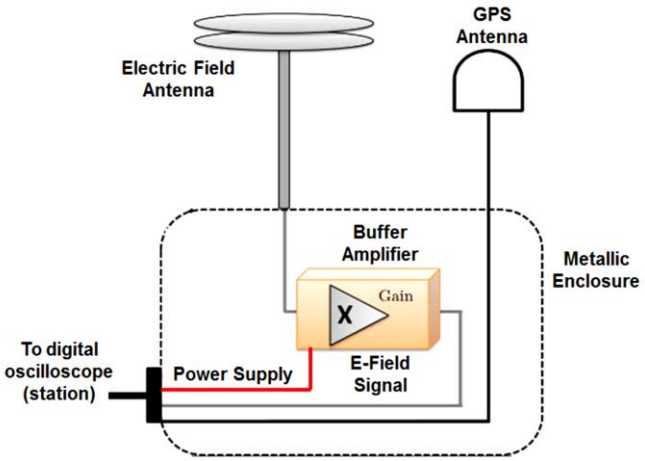

Figure 1. Lightning electric field measuring system

The electric field antenna is formed by two circular 0.45 m diameter metallic parallel plates with a 0.03 m air gap between them, supported by insulating elements. The corresponding electronic circuit is a buffer amplifier LH0033, with 100 MHz bandwidth and 1.5 kV/μs slew rate. In addition, an attenuator with a value of -20dB is used at the circuit input to avoid inconveniences when measuring near lightning signals.

The electronic circuit is connected to the antenna by means a shielded coaxial cable RG58/U. Another 20 m length coaxial cable between the electronic circuit and the measuring station was used. To acquire the signals a digital store oscilloscope is connected to the electronic circuit by means the large coaxial cable. The data were recorded at the rate of 2.5MS/s (sampling time of 400 ns) with a window size of 100 ms.

IV. Methodology

To get a comparative idea about the temporal features and the frequency spectrum of lightning electric field signatures, a set of six signals recorded from negative cloud-to-ground lightings were processed using the LPFT. These signals, corresponding to first and subsequent strokes, were extracted from different flashes. All test signals have $N = 1000$ samples with a sampling time $T_S = 400\ ns$.

In order to compare the energy concentration of each signature under study, the return strokes signals were analyzed using a window size of 200 ms. This observation window allows to analyze the complete activity of the first return stroke and the subsequent return strokes. Recorded signals were not normalized because information about the location of the negative return strokes was not available. However, according to the characteristics of the registered electric field signals and comparing them with several electromagnetic return stroke models, as it is described in [14], the lightning return strokes presented in this work were located between 15 to 50 km.

The selected signatures of the electric fields generated by lightning returns strokes have been computed with the LPFT. The LPPs are obtained using a computational application developed by authors. In this paper, the polynomial order for the LPFT computation was $m = 2$. This polynomial order was selected to reduce the computational complexity, because when m increases the number of operations also increases [8]. In all cases, a normalized rectangular windowing function is used with a bandwidth $h = 100$ samples (duration of 40 μs). Finally, in order to compare the results provided by the LPFT, a time-frequency analysis applying the STFT is also presented. For this case, STFT was calculated using the LPFT and LPP definitions presented in (2) and (6) with m=1.

V. Signal Processing And Discussion

Fig. 2 and Fig 3 show some examples of lightning electric field signatures in time domain and their LPFT power spectrums (LPP) for a first return stroke and a subsequent return stroke, respectively. The upper plots in these figures show the lightning event in time domain and the lower plots show the LPP calculated with the LPFT for m=1 (STFT) and m=2. In each upper plot (Fig. 2a and Fig 3a), the vertical axes represent the electric field magnitude whereas for the remaining plots the vertical axes represent the frequency. In all plots the horizontal axes represent the time. The amplitude of the power spectrum E^2 in $[V/m]^2$ is represented by the color scale shown in the bar located at the right side of the lower plots.

Due to the fact that all negative return stroke signals analyzed in this paper were produced by intermediate and far lightning flashes, they present a large pulse with positive polarity (under the noise components) called the initial stage. The second portion, called overshoot, is the negative polarity pulse following the initial stage [6]. The overshoot indicates that the radiation component dominates and it is predominant in the radiation of lightning [15].

In both figures (Fig. 2 and Fig 3), it is possible to observe several zones of high energy concentration. These zones are related to the return stroke activity and they are surrounded by regions where the LPP amplitude begins to decrease. These regions, in which the energy components decrease, are related to edge effects of the windowing function and small or zero values present in the computation of the LPP, and they are questionable data. For this reason, to avoid interpretation errors, the frequency range analyzed was limited between 10% and 100% of the maximum value of the power spectrum.

It is seen in Fig. 2(b) that the first return stroke spectrum computed with the STFT has frequencies form low components up to 28 kHz and the power peak of this return stroke is not located in a determined frequency. However, the peak value of

periodogram is located inside of a limited frequency range (spread distribution), which varies in time. In this case, the power spectrum peak is about of 76 $[V/m]^2$ between 500 Hz and 2.5 kHz, in a time interval of 59.6 μs to 63.2 μs.

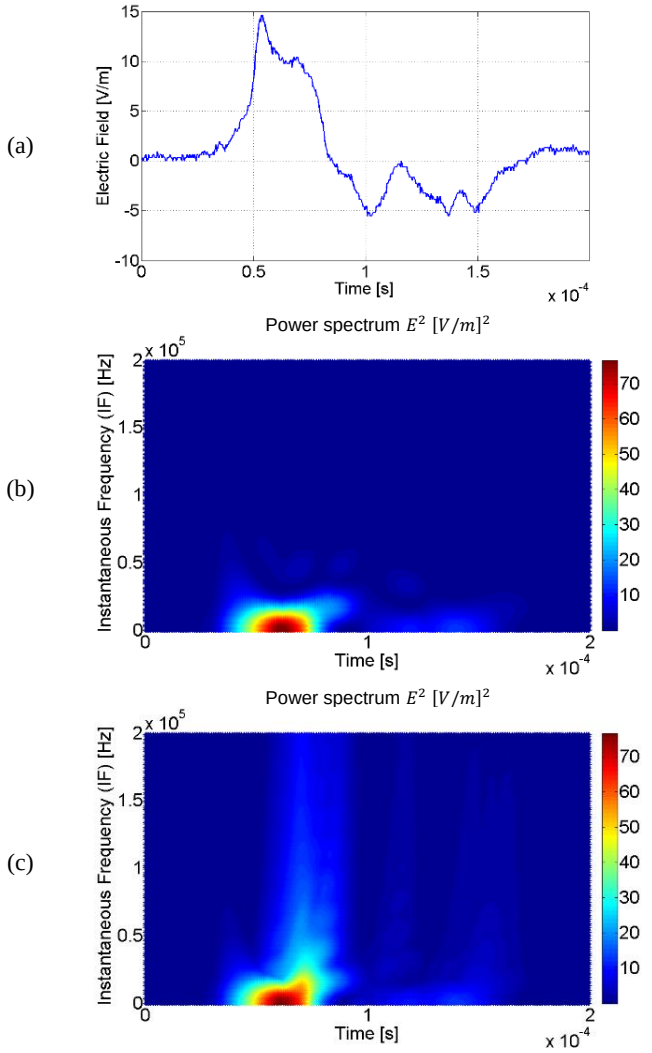

Figure 2. Example of electric field for a negative first return stroke (a) waveform in time domain (b) periodogram computed by STFT (c) LPP computed by LPFT with m=2

Fig. 2(c) shows that the second order LPFT can provide a better resolution than the method based in the conventional Fourier technique (STFT). Using LPFT, the peak value spectrum was observed from 1 kHz up to 3 kHz and located between 59.6 μs and 63.2 μs. Besides, the LPP reveals additional frequency components from 500 Hz up to about 42 kHz (between 64 μs and 84 μs) which are located in the ramp before the overshoot. These results show that the first return stroke signature preserves a low frequency content associated to the electrostatic component. Due to the difference between the amplitude of the positive peak and the overshoot (negative peak), the spectrum located in the time interval of 100 μs to 175 μs presents a lower power content. This behavior was also observed for the other negative first strokes.

In Fig. 3, the waveform of a subsequent return stroke and its corresponding periodogram and LPP are presented. It is possible to note some differences between the signal in time domain and its spectrum. In this case, the ratio between the positive and the negative peak (overshoot) is less than 2.3. For this reason, it is possible to identify the power spectrum of the overshoot region in both the periodogram and the LPP.

For the subsequent stroke cases, the best results are also achieved with the time-frequency representation provided by LPFT. By comparing Fig. 3(b) with Fig. 3(c), a remarkable difference between 75 μs and 100 μs is observed in the power spectrum. While the spectrum computed with STFT reveals a frequency content between low frequency up to 20 kHz, the LPP shows a frequency spectrum from about 500 Hz up to about 76 kHz.

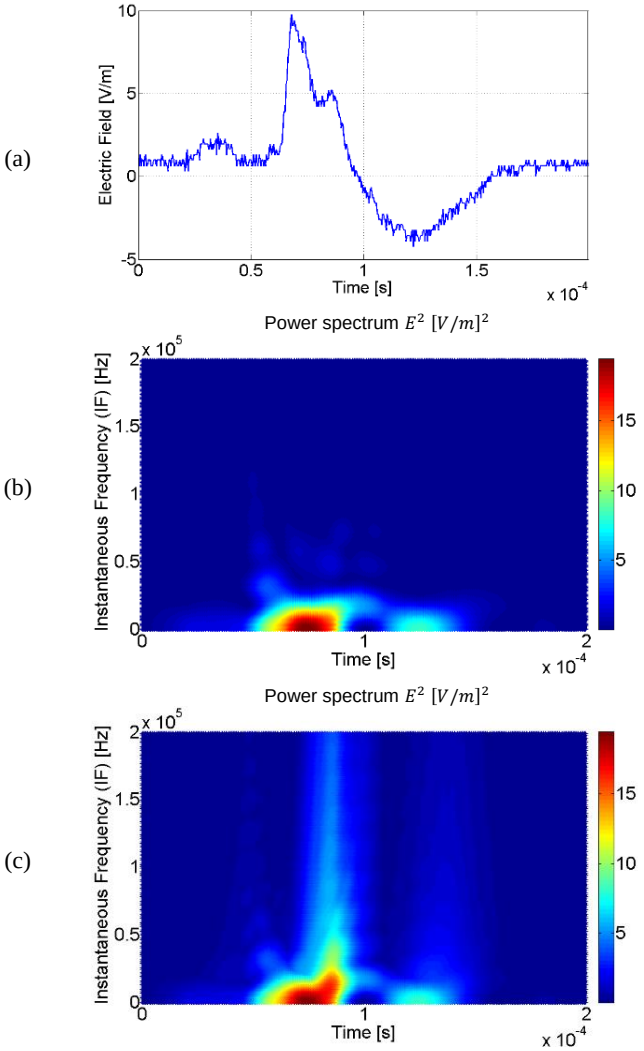

Figure 3. Example of electric field for a negative subsequent return stroke (a) waveform in time domain (b) periodogram computed by STFT (c) LPP computed by LPFT with m=2

Fig. 3(c) shows that during the initial stage, most of the energy content is located from low frequencies (related with the electrostatic component) up to about 20 kHz. Besides, the

frequency content related to the first stage and the ramp is stronger than the frequency content related to the overshoot. These results prove that the STFT allows to know the relation between time-frequency. However, it is not possible to observe medium and high frequency components present in the signal due to oscillations, ripples and changes of polarity. The main differences between the spectrum provided by STFT and the LPP (computed using the LPFT) are presented in the ramp located between the initial stage and the overshoot.

Table 1 and Table 2 present the quantitative results of the LPP power spectrum for first strokes and subsequent strokes signatures, respectively. Following the methodology presented by Sharma *et al.* [1], the parameters selected for the time-frequency analysis using the LPFT were the minimum and maximum values of the spectral range and power peak for initial stage, ramps, and overshoot, and ratio between power peaks (for each waveform).

In this way, comparing the information about the initial stage for both first and subsequent return strokes, it can be seen that the average spectral range for first stroke signatures is found to be 0.5-23 kHz, whereas for subsequent strokes is found to be 0.5-19 kHz. In both cases the low frequency radiation is notorious. For the ramp, the average spectral range was 0.5-36 kHz for negative first strokes, while for subsequent strokes the frequency range was about 0.5-42 kHz. Finally, in the case of the overshoot, the spectrum for first strokes was about 0.5-11 kHz, whereas for subsequent return strokes are found in the average frequency range of 0.5-8 kHz.

These results show that the overshoot region is located in a frequency range lower than the initial stage. However, in both cases (first and subsequent strokes) the ramp presents a spectral range above the initial stage zone. For all signatures under study it is possible to observe that the power peak of the ramp is stronger than the peak of the initial stage and the overshoot region.

On the other hand, the overshoot spectrum presents a different behavior between the first stroke and the subsequent strokes. In the case of first return strokes, the peak energy radiated by overshoot is less than that of the initial stage with an average ratio of 1:11. This ratio is reduced for subsequent stroke signatures with an average value of 1:3. For this reason, on first return stroke signals the power spectrum of the overshoot region is covered by the low frequency content.

TABLE I. RESULTS OF THE LPP SPECTRUM FOR NEGATIVE FIRST RETURN STROKES

Signal	Spectral range for the initial stage (kHz)	Power peak for the initial stage $[V/m]^2$	Spectral range for ramp (kHz)	Power peak for the ramp $[V/m]^2$	Spectral range for the overshoot (kHz)	Power peak for the overshoot $[V/m]^2$	Ratio between power peak of initial range and overshoot
Bog0_st1	0.5 - 18	63.1	0.5 - 42	76.2	0.5 - 12	5.4	11.68
Bog1_st1	0.5 - 28	16.3	0.5 - 34	26.1	0.5 - 9	1.6	10.19
Bog2_st1	0.5 - 23	21.7	0.5 - 32	30.5	0.5 - 11	2.1	10.33

TABLE II. RESULTS OF THE LPP SPECTRUM FOR NEGATIVE SUBSEQUENT RETURN STROKES

Signal	Spectral range for the initial stage (kHz)	Power peak for the initial stage $[V/m]^2$	Spectral range for ramp (kHz)	Power peak for the ramp $[V/m]^2$	Spectral range for the overshoot (kHz)	Power peak for the overshoot $[V/m]^2$	Ratio between power peak of initial range and overshoot
Bog0_st2	0.5 - 20	15.7	0.5 – 64	19.2	0.5 - 11	8.1	1.94
Bog1_st3	0.5 - 22	10.4	0.5 - 42	12.2	0.5 - 8	4.2	2.48
Bog2_st3	0.5 - 16	2.2	0.5 - 38	3.1	0.5 - 5	0.6	3.67

VI. CONCLUSIONS

In this paper, the application of the local polynomial Fourier transform (LPFT) to electric field signatures was presented. Results show that, compared with conventional techniques as STFT, it is possible to improve the instantaneous frequency (IF) estimation over lightning electric field signals generated by first and subsequent strokes. The main differences between the spectrum provided by STFT and the second order LPP (computed using the LPFT) are observed in the ramp located between the initial stage and the overshoot. Application examples using the LPFT present this technique as a potential tool for analyzing the frequency spectra of different events related with lightning phenomena.

Application of LPFT on negative first return strokes and subsequent return strokes reveals that intermediate lightning flashes present an average spectrum from lower frequencies (below 1 kHz) up to 42 kHz. These results are in agreement with the electromagnetic models for lighting flashes recorded at distances between 15 km to 50 km. However, for the initial stage and the overshoot region of the transient pulse, the first return stroke signatures present a frequency range slightly higher than those of the subsequent return strokes.

ACKNOWLEDGMENT

Authors would like to acknowledge Universidad Distrital Francisco José de Caldas for the financial support to carry out this study through the research project with code 2-5-355-13 and the commission contract N° 000002-2016. Universidad Nacional de Colombia is also acknowledged for providing the infrastructure for mounting the electric field measuring system.

REFERENCES

[1] S. R. Sharma, V. Cooray, M. Fernando, and F. J. Miranda, "Temporal features of different lightning events revealed from wavelet transform," *J. Atmos. Solar-Terrestrial Phys.*, vol. 73, no. 4, pp. 507–515, Mar. 2011.

[2] V. Cooray, "The Mechanism of the Lightning Flash," in *The Lightning Flash*, London: IEE Power Engineering Series, 2003, pp. pp. 127–240.

[3] M. J. Islam and A. M. Hussein, "Frequency domain approach to de-noise the CN Tower lightning derivative signal and its parameters calculations," *J. Comput. Electr. Eng.*, vol. 1, no. 3, pp. 328–333, 2009.

[4] U. Sonnadara, V. Cooray, and M. Fernando, "The Lightning Radiation Field Spectra of Cloud Flashes in the Interval From 20 kHz to 20 MHz," *IEEE Trans. Electromagn. Compat.*, vol. 48, no. 1, pp. 234–239, Feb. 2006.

[5] A. Poularikas, *The Transforms and Applications Handbook*, Second edi. San Francisco, USA: IEEE Press, 2000.

[6] F. J. Miranda, "Wavelet analysis of lightning return stroke," *J. Atmos. Solar-Terrestrial Phys.*, vol. 70, no. 11–12, pp. 1401–1407, 2008

[7] V. Katkovnik, "A new form of the Fourier transform for time-varying frequency estimation," in *Proc URSI International Symposium on Signals Systems and Electronics ISSSE 95*, 1995, pp. 179–182.

[8] X. Li, G. Bi, S. Stankovic, and A. M. Zoubir, "Local polynomial Fourier transform: A review on recent developments and applications," *Signal Processing*, vol. 91, no. 6, pp. 1370–1393, Jun. 2011.

[9] I. Djurovic, "Robust Adaptive Local Polynomial Fourier Transform," *IEEE Signal Process. Lett.*, vol. 11, no. 2, pp. 201–204, Feb. 2004.

[10] V. Katkovnik, "Discrete-time local polynomial approximation of the instantaneous frequency," *IEEE Trans. Signal Process.*, vol. 46, no. 10, pp. 2626–2637, 1998.

[11] V. Katkovnik, "Local polynomial periodograms for signals with the time-varying frequency and amplitude," *1996 IEEE Int. Conf. Acoust. Speech, Signal Process.*, vol. 3, pp. 1399–1402, 1996.

[12] V. Katkovnik, "Nonparametric estimation of instantaneous frequency," *IEEE Trans. Inf. Theory*, vol. 43, no. 1, pp. 183–189, 1997.

[13] H. E. Rojas, C. A. Cortés, and F. Santamaría, "Noise Reduction of Lightning Electric Fields Measurements Using Filtering in the Fractional Fourier Domain," in *7th Asia-Pacific International Conference on Lightning - APL 2011*, 2011, pp. 767–775.

[14] Y. T. Lin, M. A. Uman, J. A. Tiller, R. D. Brantley, W. H. Beasley, E. P. Krider, and C. D. Weidman, "Characterization of lightning return stroke electric and magnetic fields from simultaneous two-station measurements," *J. Geophys. Res.*, vol. 84, no. C10, p. 6307, 1979.

[15] V. A. Rakov and M. A. Uman, *Lightning: Physics and Effects*. United Kingdom: Cambridge University Press, 2007.